Concentration Fluctuations in Mixtures of Linear and Star-Shaped Polymers

T. P. Russell*

IBM Research Division, Almaden Research Center, 650 Harry Road, San Jose, California 95120-6099

L. J. Fetters

Exxon Research and Engineering Co., Corporate Research Laboratory, Annandale, New Jersey 08801

J. C. Clark, B. J. Bauer, and C. C. Han

National Institute of Standards and Technology, Gaithersburg, Maryland 20899.
Received January 20, 1989

ABSTRACT: Mixtures of linear poly(vinyl methyl ether) (PVME) with four-armed star polystyrene (PS*) were studied to evaluate the effect of chain topology on the critical fluctuations in homogeneous polymer mixtures. It was found that the cloud point curve of the PS*/PVME mixtures were elevated by ~10 °C over that of the corresponding linear mixtures. Use of deuterated PS* elevated the cloud point by another ~10 °C. Small-angle neutron scattering SANS on mixtures of the deuterated PS* with PS* was used to evaluate the single chain structure factor of the PS*. The agreement between the theories of Benoit and Burchard for branched molecules and the experimental structure factor was excellent. Using this structure factor the concentration fluctuations in the homogeneous mixtures was investigated by SANS as a function of concentration and temperature. The inverse of the intensity at zero scattering vector, $S(0)^{-1}$, extrapolated linearly with the inverse temperature to yield the spinodal temperature T_s. The correlation length, ξ, was found to depend upon $[(T - T_s)]/T_s]^{-\nu}$ where $\nu = 0.5$. ξ^{-2} was also linearly dependent on T^{-1} yielding a value of T_s at $\xi^{-2} = 0$ in close agreement with the $S(0)^{-1}$ results. ξ_0, the bare correlation length, was found to depend upon composition in a manner similar to a previous study. Finally, the Flory–Huggins interaction parameter was found to vary with $1/T$ and to depend upon composition.

Introduction

The thermodynamics and kinetics of phase separation in polymer mixtures have been of considerable theoretical and experimental interest for some time. Since the first observation of spinodal phase separation in mixtures of polystyrene PS with poly(vinyl methyl ether) (PVME) by Bank, Leffingwell, and Thies[1] and later by Nishi et al.[2] the interest in the kinetics of phase separation in polymers has surged.[3-11] This interest stems predominantly from the fact that polymer mixtures, due to the slow diffusion coefficients of polymers, are ideally suited as systems where the spinodal process can be characterized experimentally. This has not been the case for small molecule mixtures where the process occurs rapidly. In general, for polymer/polymer mixtures the initial stages of phase separation can be qualitatively described by the linearized theory of Cahn.[12-15] Modifications by de Gennes,[16] Pincus,[17] and, later, Binder[18,19] and Heerman[20] to polymers has provided some predictive capability although, only recently, quantitative comparison with theory has begun to appear.[21]

In addition to these kinetic aspects of phase separation concentration fluctuations present in the homogeneous mixtures below the lower critical solution temperature LCST have been the subject of intense interest experimentally.[22-26] Small-angle neutron (SANS) and X-ray (SAXS) scattering studies have shown that polymer mixtures can be suitably described by a mean field type behavior. As the spinodal temperature T_s is approached the correlation length ξ describing the correlations in concentration fluctuations is governed by a power law where

$$\xi = \xi_0[(T - T_s)/T_s]^{-\nu} \quad (1)$$

The exponent ν has been found to be 0.5, the mean field exponent, to within experimental error. The bare correlation length ξ_0 is found to be related to the statistical segment length of each component. In only one instance, at a composition equal to the critical composition and at temperatures very close to the critical temperature, has this relationship not proven to be valid.[27]

In this study the effect of chain topology on the phase diagram and on the concentration fluctuations is examined. The kinetic aspects of this problem will be dealt with separately.[28] Mixtures of fractionated, linear poly(vinyl methyl ether) (PVME) with a four-armed star polystyrene PS* were investigated by light scattering to evaluate the cloud point curve and by SANS to characterize the concentration fluctuations in the homogeneous mixtures below the LCST. It is shown that for these mixtures the thermodynamics is only minimally perturbed by the chain topology in that the cloud point curve is only slightly elevated. In addition, the characteristics of the zero scattering vector intensity and the correlation length are similar to that seen in linear mixtures. Finally, the Flory–Huggins interaction parameter, χ, is shown to depend upon $1/T$ and the composition of the mixture.

Experimental Section

The protonated poly(vinyl methyl ether) (PVME) ($M_w = 1.49 \times 10^5$; $M_w/M_n = 1.21$) used in this study was synthesized and fractionated as described elsewhere.[29] The synthesis of the four-armed star polystyrene molecules has been described in detail elsewhere.[30,31] The normal star polystyrene PS* had an $M_w = 2.21 \times 10^5$ with $M_w/M_n = 1.05$ whereas the deuterated star polystyrene PSD* had an $M_w = 2.11 \times 10^5$ with $M_w/M_n = 1.03$.

Cloud point measurements were performed on mixtures of PVME with linear polystyrene, PS* or PSD*, case from toluene solutions onto a microscope slide. Typically, film thick-

0024-9297/90/2223-0654$02.50/0

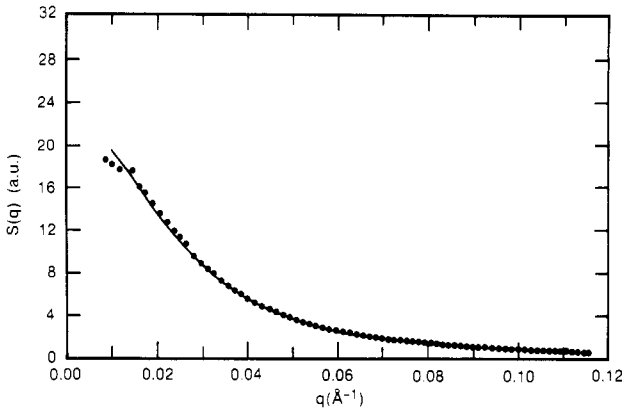

Figure 1. Small-angle neutron scattering for a mixture of 50% PSD* with 50% PS* at room temperature. The solid line through the data is a fit using the theoretical treatments of Benoit[33] and Burchard.[34]

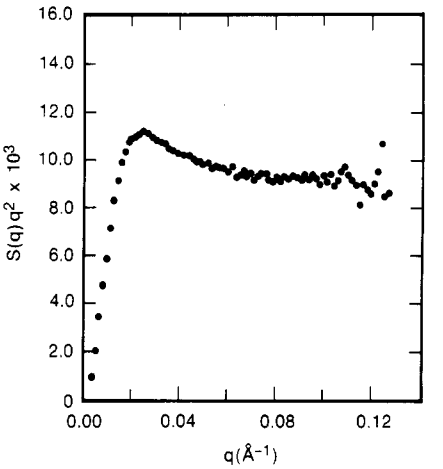

Figure 2. Kratky plot of a 25:75 PSD*/PS* mixture.

nesses of 100 μm were used. Prior to evaluation of the cloud points the mixtures were stored under vacuum at 60 °C to avoid water uptake. The cloud points were measured by using a 2-mW He–Ne laser (λ = 6328Å) with the sample mounted in a Mettler FP82 Microscopy hot stage. Both transmitted and scattered intensity were used to detect the onset of phase separation. Heating rates of 1, 5, and 10 °C/min were used. The values reported were obtained by a linear extrapolation to a zero heating rate. Despite this, however, the cloud points cannot be taken as the binodal line.

SANS studies were conducted at the National Institute of Standards and Technology. The incident neutron beam was monochromatized to 6 Å using a velocity selector. The samples were mounted into a brass heating block with aluminum windows. Temperature control was held to better than ±0.3 °C. Twelve-millimeter cadmium masks defined the size of the beam on the sample. Absolute intensity calibration was achieved by using a dry silica gel as a secondary standard that was calibrated against vanadium.[32] Mixtures of PS* and PSD* were investigated over the entire composition range to evaluate the single chain scattering function of the four-armed star molecules. These samples were prepared by freeze-drying solutions of the mixtures in benzene. The diaphanous powder was cold pressed into 1-cm pellets and then melt pressed at 150 °C into a preformed mold. Mixtures of PVME with PS* were prepared by melt pressing thoroughly dried, solution cast films of the mixtures at 110 °C. These were then placed into the heating cells and stored under vacuum at 60 °C prior to use to remove air bubbles and to prevent the uptake of water. After measurements, the samples were again stored under vacuum at 60 °C until all measurements were completed.

Results and Discussion

Prior to investigating mixtures of the PSD* with PVME the single chain scattering function of the star polymers was determined. Mixtures of PS* and the PSD* were investigated over the entire composition range. A typical scattering profile for these mixtures is shown in Figure 1. $S(q)$ is the intensity, shown here in arbitrary units, plotted as a function of the scattering vector q, which is given by $(4\pi/\lambda)\sin\theta$ where λ is the wavelength and 2θ is the scattering angle. The single chain interference function $P(q)$ for a star-shaped molecule has been shown by Benoit[33] and, later, Burchard[34] to be given by

$$P(q) = \left(\frac{2}{fv^2}\right)\left(v - (1-\exp(-v)) + \frac{f-1}{2}(1-\exp(-v))^2\right) \quad (2)$$

$$v = \frac{f}{3f-2}U^2$$

$$U^2 = q^2\langle S^2\rangle_z$$

Here, f is the functionality of the star and $\langle S^2\rangle_z$ is the mean square z-average radius of gyration. $S(q)$ and $P(q)$ are related simply through the molecular weight and contrast factor of the PS* and PSD* molecules. The solid line in Figure 1 is the result using eq 2 with $f = 4$ and $R_g = 100$ Å. Analysis of all the PS*/PSD* mixtures yielded an average value of $\langle R_g^2\rangle_z^{1/2}$ of 102 ± 2 Å. This result is in excellent agreement with the data of Roovers et al.[30,35,36] From their dilute solution light scattering measurements in a θ solvent

$$\langle R_g^2\rangle_z^{1} = 2.8 \times 10^{-1} M^{0.484} \quad (3)$$

which yields a value of $\langle R_g^2\rangle_z^{1/2} = 102$ Å for the star molecules studied here. The value of $\langle R_g^2\rangle_z^{1/2}$ for the corresponding linear polymer[30,37] is 129 Å yielding $g = (\langle R_g^2\rangle_{z,PS*}/\langle R_g^2\rangle_{z,PS})^2 = 0.63$ which is in good agreement with the results of Zimm and Stockmayer[38] and with later refinements of Daoud and Cotton[39] and Douglas and Freed.[40] Thus, the four-armed star polymers used in this study are well-defined and are described suitably by random coil statistics of these polymers in a θ solvent.

It is worthwhile to examine the scattering function of the PSD* further. In Figure 2 the data is plotted as $S(q)q^2$ vs q, i.e., as a Kratky plot. A maximum is seen at $q = 0.025$ corresponding to $U = 2.55$. This agrees remarkably well with the value of 2.52 predicted by Burchard.[34] In addition, the ratio of the intensity of the maximum, $(S(q)q^2)_{max}$, to that at higher scattering vector, $(S(q)q^2)_\infty$, is 1.17. This compares to the value of 1.14 predicted by Burchard for monodisperse star molecules. The pronounced maximum seen in Figure 2 coupled with the fact that the $(S(q)q^2)_{max}/(S(q)q^2)_\infty$ ratio was not reduced by polydispersity effects suggests that the polydispersity of the star molecules is low.

Mixtures of PS* with PVME exhibit a single glass transition temperature, T_g, as measured by differential scanning calorimetry, which is characteristic of a miscible system. The T_g of PVME was found to be −20 °C, whereas that for the PS* was 99 °C in good agreement with published values.[41] As shown by the lowest curve in Figure 3, the T_g's of the mixtures varied smoothly, though not linearly, with composition. Upon heating the mixtures to elevated temperatures phase separation occurs. The cloud points, extrapolated to a zero heating rate, are shown in Figure 3 by the solid triangles. These are similar to the results of Nishi et al.[42] It is interesting to compare this result with that obtained from the corresponding linear PS mixture with PVME where the total molecular

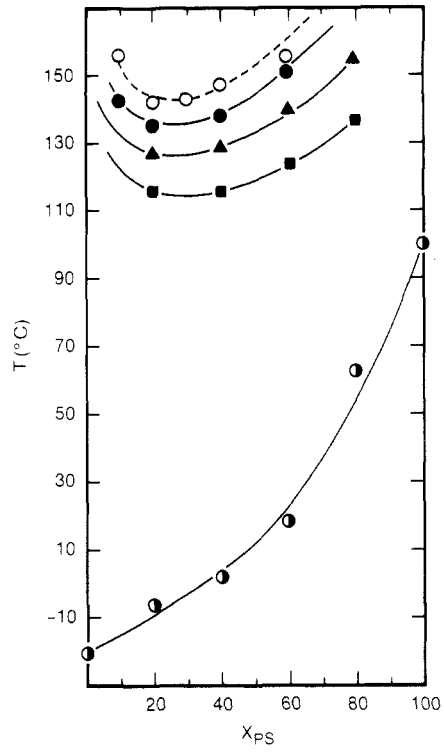

Figure 3. Cloud points for mixtures of PS (■), PS* (▲), and PSD* (●) with PVME as a function of the weight percent of polystyrene. The cloud points were extrapolated to a zero heating rate in all cases. The spinodal points (○) for PSD*/PVME mixtures were obtained by analysis of the correlation length and scattering at $q = 0$ as a function of temperature. The glass transition temperature (◑) as a function of composition for PSD*/PVME mixtures was determined at a heating rate of 20 °C/min.

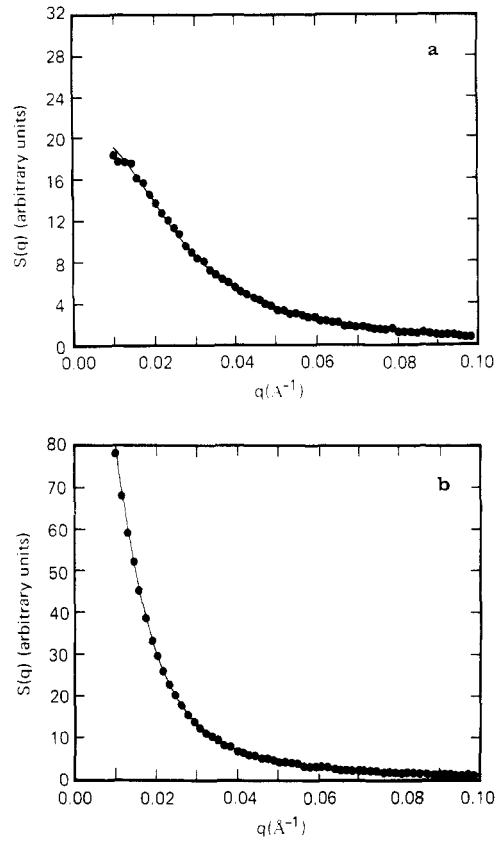

Figure 4. a. Small angle neutron scattering for a PSD*/PVME mixture (ϕ_{PSD}* = 0.189) at 100 °C. The solid line is the fit using a de Gennes function where the topology of the star as taken into account. b. Same as in a but the temperature has been changed to 136 °C. Note the five-scale increase in the abscissa reflecting the dramatic increase in scattering.

weight of the PS is kept constant. The cloud points for the linear mixtures extrapolated to a zero heating rate are indicated by the squares in Figure 3. It is seen that the cloud point curve for the linear mixtures is approximately 12° lower than that of the corresponding PS* mixtures. This temperature change is small and indicates that the perturbation of the free energy caused by the variations in the chain topology is slight. Finally, mixtures of PSD* with PVME exhibit cloud points that are somewhat (ca. 6 °C) higher than the corresponding protonated analogues. The increase in the cloud point by deuteration of one of the components has been found previously for mixtures of the two linear polymers PS/PVME.[43,44] The effect observed in this study on the PSD*/PVME mixtures is much less pronounced than that observed for the linear mixtures where an approximate 30 °C difference was found.

Neutron scattering studies were performed on the PSD*/PVME as a function of temperature at temperatures less than the observed cloud points for volume fractions of PSD*, ϕ_{PS}, of 0.095, 0.189, 0.286, 0.385, and 0.584. The lowest temperature used in any of the studies was 100 °C which, as can be seen from Figure 3, is well above the T_g of the mixtures. Typical scattering profiles for the PS*/PVME mixtures are exemplified by the $\phi_{PS} = 0.189$ mixtures of PSD* with PVME shown in Figure 4a at 100 °C and Figure 4b at 136 °C. It is evident from these data, considering the 5-fold increase in the abscissa in Figure 4b, that the neutron scattering has increased dramatically with an increase in the temperature. The scattering from a homogeneous polymer mixture was described by de Gennes[45] using the random phase approximation. From these arguments the total structure factor $S_T(q)$ is related to the structure factor of the individual components, $S_{PS}(q)$ or $S_{PVME}(q)$, by

$$S_T(q) = K_n\left\{\frac{1}{V_{PS}Z_{PS}\phi_{PS}S_{PS}(q)} + \frac{1}{V_{PVME}Z_{PVME}\phi_{PVME}S_{PVME}(q)} - \frac{2\chi}{V_0}\right\}^{-1} + C \quad (4)$$

where $S_{PS}(q)$ and $S_{PVME}(q)$ are defined in terms of the interference function in eq 2 where $f = 1$ and 4 for the PVME and PSD*, respectively. K_n is the difference in scattering length densities of the two components defined as $N_A[(a_{PSD}*/V_{PSD}*) - (a_{PVME}/V_{PVME})]^2$ where a_i is the scattering length per mole of monomer with molar volume v_i and N_A is Avogadro's number. Z_i is the degree of polymerization of component i with volume fraction ϕ_i, V_0 is a reference molar volume, and χ is the Flory–Huggins interaction parameter as measured in the scattering experiment. C is an angularly independent constant that takes into account any background contributions to the scattering, including incorrect subtraction of incoherent scattering. Over the scattering vector range of interest C was at most 10% of the total scattering at higher angles and negligible at lower angles. For measurements near the spinodal temperature the contribution of C to the total scattering was insignificant. ϕ_i, Z_i, and V_i are given in Table I for all the components, fitting eq 4 to the experimental data requires adjustment of $R_{g,PVME}$, χ, and C.

The solid lines drawn in parts a and b of Figure 4 represent the best fits of eq 4 to the experimental data. Agreement between the theoretical fit and experimental data

Table I
Parameters for Individual Components

	PSD[a]	PVME
$10^5 M_w$	2.1	1.49
M_w/M_n	1.03	1.21
Z	18.7	2570
ν, cm^3/mol	188 000	14 300
$10^{12}a$, cm/mon	10.656	0.331
ρ, g/cm^3	1.116	1.047

[a] Parameters are for perdeuterated PS.

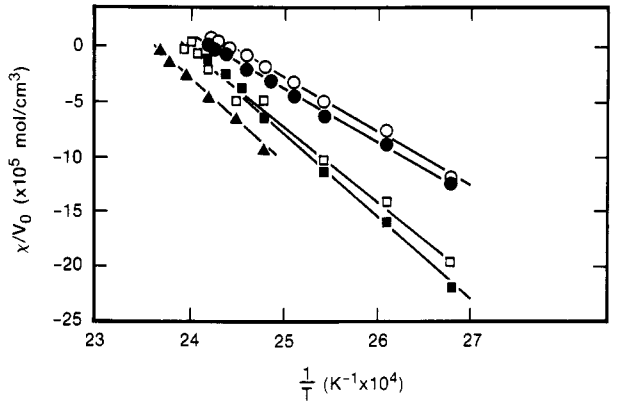

Figure 5. The interaction parameter, χ/V_0 as a function of the inverse temperature, $1/T$, for mixtures of PSD* with PVME where the volume fraction of PSD* is 0.095 (●), 0.189 (○), 0.286 (■), 0.385 (□), and 0.584 (▲).

was better than ±2.5% over the entire scattering vector range. The values of χ/V_0 obtained as a function of the reciprocal of the measurement temperature for the different compositions investigated are shown in Figure 5. For a given composition χ/V_0 is seen to vary linearly with the inverse temperature. This result has been found for numerous homopolymer mixtures as well as diblock copolymers.[46] At a given temperature, χ/V_0 also depends upon composition and appears to have a maximum value near a ϕ_{PSD^*} of ca. 0.2 as can be seen by the order of the lines in Figure 5. The compostion dependence of χ/V_0 is predicted by the more recent treatments of polymer mixtures;[47] however, quantitative comparison with these theoretical arguments would be premature at this time.

From the fitting of the temperature and composition dependent scattering $R_{g,PVME}$ was found to be essentially invariant. Shown in Table II are the average values of $R_{g,PVME}$, obtained for each composition. From these data it is also evident that $R_{g,PVME}$ did not vary significantly with composition. Averaging over all compositions a value of $R_{g,PVME}$ = 195 ± 15 Å is obtained that compares quite well with the value of 208 Å reported elsewhere[51] for PVME under θ conditions.

At a given temperature and composition the correlation length $\xi(T, \phi)$ characterizing composition fluctuations in the mixture is given by[23,45]

$$\xi^2(T,\phi) = \frac{b^2}{36\phi_A\phi_B(\chi_s - \chi)} = \frac{b^2}{36V_0\phi_A\phi_B\left(\frac{\chi_s}{V_0} - \frac{\chi}{V_0}\right)} \quad (5)$$

where χ_s is the value of χ at the spinodal temperature and b^2 is the mean square statistical segment length. Since χ varies with the inverse temperature, then ξ^{-2} should vary with T^{-1}, and at the spinodal temperature, where $\chi = \chi_s$, ξ^{-2} should be zero. This simply states that at the spinodal temperature the correlation length characterizing the concentration fluctuations become infinite in size. From the values of b and χ/V_0 obtained earlier by fitting the experimental $S_T(q)$ to eq 4, ξ can be calculated by using eq 5.

Table II
Results of Scattering Analysis for PSD*/PVME Mixtures

ϕ_{PS}	T_s,[a] °C	T_s,[b] °C	$R_{g,PVME}$,[a] Å	$(b^2)^{1/2}$,[c] Å	ξ_0, Å	γ
0.095	156.8	158.5	200	9.7	20.0	0.48 ± 0.02
0.189	143.8	143.6	186	9.0	15.8	0.51 ± 0.01
0.286	148.2	152.2	219	10.5	11.9	0.48 ± 0.04
0.385	147.6	145.9	199	9.6	12.0	0.47 ± 0.03
0.584	152.5	151.8	175	8.6	11.2	0.49 ± 0.01

[a] Evaluated from $S(0)^{-1}$ plot. [b] Evaluated from ξ^{-2} vs T^{-1} plot. [c] Evaluated by averaging over the entire temperature range studied.

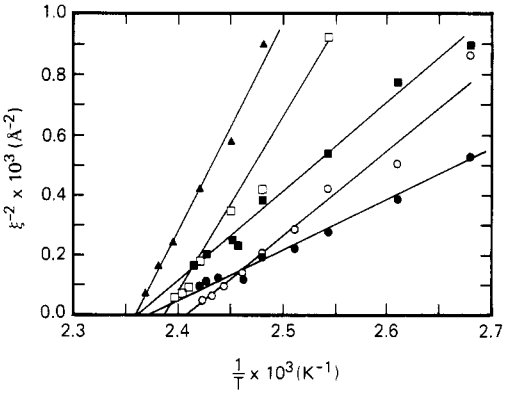

Figure 6. The inverse square correlation length, ξ^{-2}, as a function of inverse temperature, $1/T$, for PSD*/PVME mixtures where the volume fraction of PSD* is 0.095 (●), 0.189 (○), 0.286 (■), 0.385 (□), and 0.584 (▲).

The values of ξ^{-2} are shown in Figure 6 plotted as a function of inverse temperature. Throughout the entire temperature regime studied, ξ^{-2} is seen to vary linearly with inverse temperature for all compositions. Deviations from the mean field behavior, as discussed by Schwahn et al.,[27] were not observed in this experiment. From the data in Figure 6, extrapolation of ξ^{-2} to zero was straightforward yielding the value of T_s.

The values of T_s for each composition are shown in Table II and are plotted with the cloud point data in Figure 3. It is seen in Figure 3 that the locus of points defined by the cloud points and the spinodal line defined by the extrapolated of ξ^{-2} do not intersect. This can be due to the fact that the cloud points do not truly define the binodal. If so, they would be tangent to each other at the minimum. The values of T_s for each composition can also be determined from eq 5. If, as was shown, ξ^{-2} varies linearly with inverse temperature, then $S(0,T)^{-1}$ should vary as $1/T$. The extrapolated values of $S(0,T)^{-1}$ are shown in Figure 7 plotted as function of $1/T$. As can be seen, very good linearity is observed allowing a relatively simple extrapolation to $S(0,T)^{-1} = 0$. The values of T_s obtained from this analysis are shown in Table II and are seen to be in very good agreement with the previous results. Thus, the discrepancy of the nonintersection of the cloud point curve and the spinodal line must be due to the nonequilibrium nature of the cloud point curve. Regardless, both curves appear to have a minimum near ϕ_{PS} = 0.22, indicating that this is the critical composition of the mixtures.

The mean square statistical segment length for each composition, $(b^2)^{1/2}$, obtained from the nonlinear least-squares fitting of eq 4 to the data, varied by at most 10% over the temperature interval investigated. The average

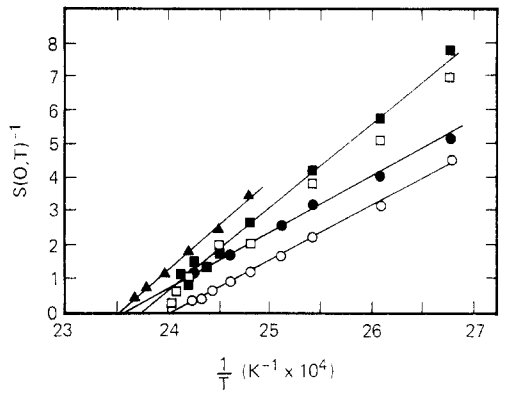

Figure 7. The inverse neutron scattering intensity extrapolated to $q = 0$, $S(0,T)^{-1}$, as a function of the inverse temperature, $1/T$, for PSD*/PVME mixtures where the volume fraction of PSD* is 0.095 (●), 0.189 (○), 0.286 (■), 0.385 (□), and 0.584 (▲).

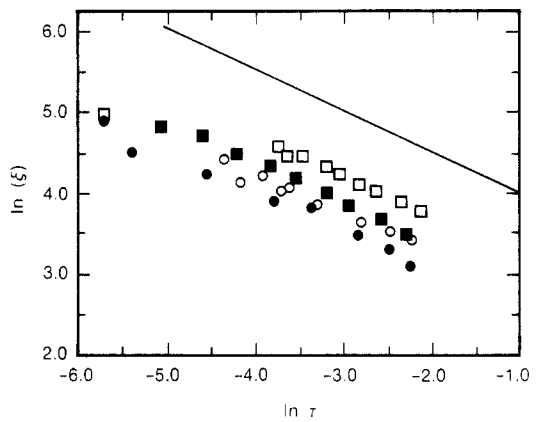

Figure 8. Logarithm of the correlation length, ξ, as a function of the reduced temperature, $\tau = (T - T_s)/T_s$, for PSD*/PVME mixtures where the volume fraction of PSD* is 0.095 (●), 0.189 (○), 0.286 (■), and 0.385 (□). The line shown has a slope of −0.5.

value for each composition is shown in Table II. As can be seen, $(b^2)^{1/2}$ does not vary markedly over the entire composition range and yields a composite average value of $(b^2)^{1/2}$ of 9.5 ± 1 Å. In comparison with mixtures of PSD and PVME investigated previously where a value of 7.7 Å, the value found here is somewhat larger. This may be associated with the topological constraints of the star molecules. However, taking into account the polydispersity of the PVME, a calculated value of $(b^2)^{1/2}$ of 8.5 was found for the linear mixtures[52] which is within the error limits of these measurements.

From mean field arguments in the limit of $T \rightarrow T_s$ the critical fluctuations should scale according to[53,54]

$$\xi(T, \phi) = \xi_0 \tau^{\gamma} \qquad (6)$$

where τ, the reduced temperature, is $(T - T_s)/T_s$ and $\xi_0(\phi)$ is the bare correlation length for a composition ϕ. The log of ξ is shown in Figure 8 as a function of the log of the reduced temperature for each of the compositions studied. For reference, a line with a slope of −0.5 is also shown. The slopes of each line, γ, and the bare correlation lengths obtained for each composition are given in Table II. As can be seen, to within experimental errors, ξ for each composition varies with $\tau^{-0.5}$; i.e., the star linear mixtures are behaving in a mean field manner over the temperature range studied. This is precisely the behavior observed for the linear/linear mixtures.

The values of the bare correlation length determined from these data are given in Table II. As can be seen ξ_0 decreases with increasing PSD* concentration. These values of ξ_0 are only slightly larger than the values of ξ_0 determined for the linear/linear mixtures. In both cases a similar concentration dependence is found. On the basis of these results, it is clear that the topological changes have not dramatically altered the range over which interactions occur in these systems. In fact, the overall thermodynamic behavior of the star polymers is remarkably similar to that of their linear counterparts. This, however, does not appear to be the case when the number of arms in the star polymer becomes very large.[55]

In conclusion, the data presented here show that the configuration of four-armed star polystyrene molecules can be well described by the theoretical arguments of Benoit[33] and Burchard[34] for branched polymer systems. The cloud point for the star molecule mixtures with PVME is elevated by ~10 °C over that of the linear/linear mixtures, whereas deuteration of the star molecules elevates the cloud point by ~10 °C further. This effect of deuteration is much less than that observed for the linear/linear mixture. Mean field arguments appear to describe the behavior of the PSD*/PVME mixtures quite well. The data yield χ that varies with composition, a mean statistical segment length that is in agreement with calculated values, and a bare correlation length that varies with composition. The correlation length varies with a reduced temperature with a 0.5 exponent as predicted for mean field type systems. The PSD*/PVME mixtures can be characterized by virtually the same parameters as are used for their linear counterparts indicating that the chain topology does not perturb the thermodynamics of the mixtures significantly.

References and Notes

(1) Bank, M.; Leffingwell, J.; Thies, J. *J. Polym. Sci.* **1972**, *10*, 1097.
(2) Nishi, T.; Wang, T. T.; Kwei, T. K. *Macromolecules* **1975**, *8*, 277.
(3) Snyder, H. L.; Meakin, P.; Reich, S. *Macromolecules* **1983**, *16*, 757.
(4) Gelles, R.; Frank, C. W. *Macromolecules* **1982**, *15*, 1486.
(5) Hashimoto, T.; Kumaki, J.; Kawai, H. *Macromolecules* **1983**, *16*, 641.
(6) Hashimoto, T.; Izumitani, T. *J. Chem. Phys.* **1985**, *83*, 3694.
(7) Russell, T. P.; Hadziioannou, G.; Warburton, W. *Macromolecules* **1985**, *18*, 78.
(8) Ronca, G.; Russell, T. P. *Macromolecules* **1985**, *18*, 665.
(9) Strobl, G. *Macromolecules* **1985**, *18*, 558.
(10) Gilmer, J.; Goldstein, N.; Stein, R. S. *J. Polym. Sci., Polym. Phys. Ed.* **1982**, *20*, 2219.
(11) Reich, S.; Cohen, Y. *J. Polym. Sci., Polym. Phys. Ed.* **1981**, *19*, 1255.
(12) Cahn, J. W. *J. Chem. Phys.* **1965**, *42*, 93.
(13) Hilliard, J. E. In *Phase Transformations*; American Society of Metallurgy, Oct 1968, p 497.
(14) Cahn, J. W. *Trans. Am. Inst. Min., Metall., Pet. Eng., Soc. Min. Eng. AIME* **1968**, *242*, 166.
(15) Cook, H. E. *Acta Metall.* **1970**, *18*, 297.
(16) de Gennes, P. G. *J. Chem. Phys.* **1980**, *72*, 4756.
(17) Pincus, P. *J. Chem. Phys.* **1981**, *75*, 1996.
(18) Binder, K. *J. Chem. Phys.* **1983**, *79*, 6387.
(19) Binder, K. In *Kinetics of Aggregation and Gelation*; Family, F., Landau, P. P., Eds.; Elsevier: Amsterdam, 1984; p 209.
(20) Heermann, D. W. *Phys. Rev. Lett.* **1984**, *52*, 1126.
(21) Sato, T.; Han, C. C. *J. Chem. Phys.* **1988**, *88*, 2057.
(22) Herkt-Maetzky; Schelten, J. *Phys. Rev. Lett.* **1983**, *51*, 896.
(23) Shibayama, M.; Yang, H.; Stein, R. S.; Han, C. C. *Macromolecules* **1985**, *18*, 2179.
(24) Yang, H.; Shibayama, M.; Stein, R. S.; Han, C. C. *Polym. Bull. (Berlin)* **1984**, *12*, 7.
(25) Joanny, J. F. *C. R. Sceances Acad. Sci., Ser. B.* **1978**, *286*, 89.
(26) Ronca, G.; Russell, T. P. *Phys. Rev. B* **1987**, *35*, 8566.
(27) Schwahn, D.; Mortensen, K.; Yee-Madeiru, H. *Phys. Rev. Lett.* **1987**.
(28) Factor, B. J.; Smith, B. A.; Russell, T. P.; Fetters, L. J.; Han, C. C., submitted for publication.

(29) Bauer, B. J.; Hanley, B.; Muroga, Y. *Polym. Commun.* **1989**, *30*, 19.
(30) Roovers, J. E. L.; Bywater, S. *Macromolecules* **1972**, *5*, 385.
(31) Bauer, B. J.; Fetters. L. J. *Rubber Chem. Technol.* **1978**, *52*, 406.
(32) Glinka, C., private communication.
(33) Benoit, H. *J. Polym. Sci.* **1953**, *11*, 561.
(34) Burchard, W. *Macromolecules* **1977**, *10*, 919.
(35) Roovers, J.; Bywater, S. *Macromolecules* **1974**, *7*, 443.
(36) Roovers, J.; Toporowski, P. M. *J. Polym. Sci., Polym. Phys. Ed.* **1980**, *18*, 1907.
(37) Schmidt, M.; Burchard, W. *Macromolecules* **1981**, *14*, 210.
(38) Zimm, B. H.; Stockmayer, W. H. *J. Chem. Phys.* **1949**, *17*, 1301.
(39) Daoud, M.; Cotton, J. P. *J. Phys. (Les Ulis, Fr.)* **1982**, *43*, 531.
(40) Douglas, J. F.; Freed, K. F. *Macromolecules* **1984**, *17*, 2344.
(41) van Krevelen, D. W. *Properties of Polymers*: Elsevier: Amsterdam, 1976.
(42) Nishi, T.; Wang, T. T.; Kwei, T. K. *Macromolecules* **1975**, *8*, 227.
(43) Yang, H.; Hadziioannou, G.; Stein, R. S. *Sci. Phys. Ed.* **1983**, *21*, 159.
(44) Halary, J. L.; Ubrich, J. M.; Monnerie, L.; Yang, H.; Stein, R. S. *Polym. Commun.* **1985**, *26*, 73.
(45) de Gennes, P. G. *Scaling Concepts in Polymer Physics*; Cornell University Press: New York, 1979; Chapter IV.
(46) Owens, J. N.; Koberstein, J. T.; Gancarz, I.; Russell, T. P. *Macromolecules*, accepted for publication.
(47) Sanchez, I. C.; Lacombe, R. H. *J. Phys. Chem.* **1976**, *80*, 2352.
(48) Lacombe, R. H.; Sanchez, I. C. *J. Phys. Chem.* **1976**, *80*, 2568.
(49) Eichinger, B.; Flory, P. J. *Trans. Faraday Soc.* **1968**, *64*, 2038.
(50) Flory, P. J. *Discuss. Faraday Soc.* **1970**, *49*, 7.
(51) Brandrup, J., Immergut, E. H., Eds. *Polymer Handbook*; Wiley: New York, 1975.
(52) Hashimoto, T. *Current Topics in Polymer Science*; Ottenbrite, R. M., Utracki, L. A., Inoue, S., Eds.; Hanser Publishers: Munich, 1987; Vol. II, p 199.
(53) Stanley, H. E. *Introduction to Phase Transitions and Critical Phenomena*; Oxford University Press: New York, 1971.
(54) de Gennes, P. G. *J. Phys. (Les Ulis, Fr.)* **1977**, *38*, L-441.
(55) Gilmer, J. W.; Bringuier, A. G.; Sremcich, P. S. *Macromolecules*, submitted for publication.

Registry No. PVME, 9003-09-2; PS, 9003-53-6.

Tracer Diffusion of Linear Polystyrene in Entanglement Networks

Norio Nemoto,* Masahiro Kishine, Tadashi Inoue, and Kunihiro Osaki

Institute for Chemical Research, Kyoto University, Uji, Kyoto-fu 611, Japan.
Received March 29, 1989; Revised Manuscript Received June 26, 1989

ABSTRACT: The tracer diffusion coefficient D_{tr}^{∞} of linear polystyrenes (PS) with weight-average molecular weights M_w from 6100 to 2 890 000 was measured in entanglement networks of PS with M_ws much higher than the molecular weight of the respective diffusants at temperature of 30 °C by using forced Rayleigh scattering technique. Total polymer concentration C was 13 and 18 wt %, and C of the diffusant was fixed at 1 wt %. Dibutyl phthalate was used as solvent. D_{tr}^{∞} data at C = 13 and 18 wt % and also those obtained at 40.6 wt % in an earlier study were found to be superposed on one master curve by using two parameters, an effective friction coefficient of a segment ζ and the molecular weight between entanglements M_e, for reduction. Reduced D_{tr}^{∞} was proportional to M^{-1} and $M^{-2.5}$ in the unentangled ($M/M_D < 1$) and the entangled region ($M/M_D > 1$), respectively, where M_D is the molecular weight at the intersection point and is very close to M_e.

Introduction

In a previous study,[1] the tracer diffusion coefficient D_{tr} of linear polystyrenes (PS) with molecular weights M_N was measured in entanglement networks of matrix PS with molecular weights M_P in the concentrated regime by using the forced Rayleigh scattering technique. We found that D_{tr} asymptotically took a value of D_{tr}^{∞} independent of the molecular weight M_P of PS matrix with $M_P > 5M_N$, and also that D_{tr}^{∞} obtained exhibited a break at a characteristic molecular weight M_D, which was very close to the molecular weight between entanglements M_e of the network. D_{tr}^{∞} was inversely proportional to M_N below M_D, which indicates that the diffusing chain can be pictured as a free-draining Rouse chain with an effective segment friction coefficient of $\zeta(C,T)$. Above M_D, the dependence of D_{tr}^{∞} on M_N was expressed by the power law $D_{tr}^{\infty} \propto M_N^{-\alpha}$ with the exponent α = 2.5 for the largest value of M_N/M_e = 30 studied. This behavior is in contrast to the tracer diffusion behavior in melts[6] where α is very close to 2, in agreement with the prediction of the reptation theory.[17] A similar difference in the exponent α between concentrated solutions and melts was also observed for self-diffusion behavior.[1,2-9] Thus the retardation effect on diffusion due to the elastic entanglement network characterized by M_e appeared stronger in the concentrated regime than in melts.

In the semidilute regime, there are large amounts of self-diffusion and tracer diffusion data.[23-31] Among them, the most extensive study on D_{tr}^{∞} behavior made by Yu and co-workers[10] showed that D_{tr}^{∞} exhibited quite strong molecular weight dependence, such that α may be close to 3. Then acceptance of all values of the exponents reported leads to supposition that the exponent tends to monotonically decrease with increasing concentration from a value of 3 in the semidilute regime to 2 in melts. However, we may point out that exponents for concentrated solution and melt data were obtained in the highly entangled region of $M_N/M_e > 10$, whereas a maximum value of M_N/M_e attained is less than 10 for semidilute solution data. Therefore there remains an ambiguity with respect to the exponent 3, which is only apparent and decreases with increasing M_N/M_e toward a somewhat lower value at large M/M_e values as is observed for melt data. It should be also noted that the exponent α for the self-diffusion coefficient D_s in the semidilute regime is not in complete agreement with the theoretical value of 2 but appears to be near 2.

The present investigation is first aimed at extending D_{tr}^{∞} measurements in the semidilute regime to the region

0024-9297/90/2223-0659$02.50/0